Available online at www.sciencedirect.com
ScienceDirect
Journal of Sound and Vibration 316 (2008) 87–100
JOURNAL OF SOUND AND VIBRATION
www.elsevier.com/locate/jsvi

Estimation of complex Young's modulus of non-stiff materials using a modified Oberst beam technique

Yabin Liao*, Valana Wells

Department of Mechanical and Aerospace Engineering, Arizona State University, P.O. Box 876106, Tempe, AZ 85287-6106, USA

Received 17 July 2007; received in revised form 16 January 2008; accepted 19 February 2008
Handling Editor: P. Davies
Available online 2 April 2008

Abstract

The paper presents a modified Oberst beam technique to evaluate the complex Young's modulus of non-stiff materials. Unconstrained layer theories and non-parametric complex modulus identification methods used for stiff materials form the basis for the method. The proposed approach has several advantages over the standard Oberst beam technique. In particular, the layer properties can be evaluated at any frequency, and the base beam need not be completely covered with the layer material. In addition, the proposed method does not require that the complex modulus vs. frequency curve for the base beam should have a flat area near analyzed resonance frequencies in order to yield accurate results. The experiments conducted on a styrene–butadiene rubber (SBR) sample using a polymethyl methacrylate (PMMA) base beam produced good results. Uncertainty analysis shows that the measurement accuracy can be improved by increasing the modulus magnitude ratio between the layer material and the base beam material, or the thickness ratio between the layer and base beam.

1. Introduction

Since the 1950s, various experimental techniques have been developed to determine the complex Young's modulus of viscoelastic solids [1–9]. Many of these methods have utilized tests involving vibrating beams because of their simplicity in both theory and experimental setup. The conventional vibrating-beam techniques either exploit the modal characteristics of the beams, or are based on the propagating wave model. However, the former group of methods can only evaluate the complex modulus at resonance frequencies and, to obtain accurate results, the damping must be small. Moreover, the conventional methods depend on specific boundary conditions that might not be easy to achieve in practice, especially for the methods utilizing propagating wave theory.

Recently several complex modulus measurement techniques have been proposed to overcome these disadvantages. These techniques and their associated analysis are non-parametric in the sense that the complex modulus identification process does not rely on boundary conditions. Based on the propagating wave model,

*Corresponding author. Tel.: +1 480 965 3668.
E-mail address: Yabin.Liao@asu.edu (Y. Liao).

0022-460X/$ - see front matter © 2008 Elsevier Ltd. All rights reserved.
doi:10.1016/j.jsv.2008.02.028

they can continuously measure the complex modulus in a wide frequency range not restricted to resonance frequencies, and they do not depend on boundary conditions as long as the beam model assumptions are satisfied.

Hull and Hurdis [10] showed that the complex modulus could be exactly determined from five transfer functions measured at evenly spaced locations on the test beam. Hillström, Mossberg and Lundberg proposed a complex modulus estimation method using least squares [11]. The least squares (LS) method first assumes a tentative wavenumber, uses the classical LS algorithm to reconstruct an optimized wave field, and calculates the mean square error between the optimized and measured wave fields. Then the process is repeated for new wavenumbers until the mean square error is minimized and the corresponding wavenumber is taken as the identified wavenumber, from which the complex modulus is calculated.

More recently, Liao and Wells [12] developed an estimation method using wave coefficients. Based on the propagating wave model of uniform beams, the Wave Coefficients (COE) method seeks a wavenumber that forces the measurement points to have, as close as possible, the same wave coefficients. The COE method follows a procedure similar to that of the LS method: first a tentative wavenumber is assumed; and then sets of wave coefficients are calculated from different combinations of wave field measurements on the test beam, and the error among these sets of wave coefficients is computed; the process then uses an optimization technique to find the wavenumber that minimizes the wave coefficient error. The complex modulus can then be calculated from the identified wavenumber.

Liao and Wells applied the COE and LS methods to stiff materials such as aluminum and polymethyl methacrylate (PMMA). A laser vibrometer was used to obtain accurate vibration velocity measurements on the beam. The results are in good agreement with those obtained by more conventional methods and with those previously published over most of the frequencies of interest, 30–800 Hz.

However, if the test material is not stiff enough to support itself, it cannot be formed into a beam, and the complex modulus estimation methods cannot be directly applied. Most practical damping materials fall into the classification of ''non-stiff'' [2,5,13]. Layer theories have been developed to indirectly measure properties of damping-type materials [3,5,13–16]: the soft material layer can be coated on a stiff base beam (as in an unconstrained layer configuration) or be sandwiched between stiff materials (as in a constrained layer configuration). The effective complex modulus of the composite beam is estimated using the complex modulus measurement techniques for stiff materials, and finally the soft material properties can be extracted from the effective properties utilizing the layer theory.

The most well known of the unconstrained-layer-based methods is the standard Oberst beam technique [1,5,13,15], which is based on the Oberst equation [15] for unconstrained layer systems. Since it uses conventional modal testing to determine the complex modulus of the stiff base beam and the effective complex modulus of the composite beam, it is subject to the same restrictions as the conventional complex modulus measurement techniques, that is, the layer properties can only be evaluated at resonance frequencies, and the layer material must completely cover one surface of the base beam.

In addition to the above limitations, it is also necessary that the complex modulus vs. frequency function for the base beam should have minimal slope near analyzed resonance frequencies. This point is illustrated in Fig. 1, which shows a fit curve from actual storage modulus measurements of PMMA. For discussion purposes, assume f_{01} and f_{02} are two measured resonance frequencies of the base PMMA beam, and f_1 and f_2 are the resonance frequencies of the composite beam with coated damping layers. As will be discussed in more detail in Section 2, the standard technique estimates the complex modulus of the base beam at resonance frequency, f_{01}. The method then uses the beam properties at this frequency to evaluate the complex modulus of the layer at its natural frequency f_1. A large variation in complex modulus between f_{01} and f_1 leads to large errors in the layer property extraction. On the other hand, if the complex modulus curve between base and composite beam resonance frequencies has zero or near-zero slope, as between f_{02} and f_2, using the base beam properties at f_{02} to extract layer properties at f_2 leads to very accurate results.

Wojtowicki et al. [17] addressed some of the difficulties and uncertainties associated with the boundary condition setup for conventional Oberst beam testing. By shaking a beam at its midpoint, they took advantage of the symmetry of the system to enforce zero slope at the center thereby allowing either half of the beam to be modeled with clamped-free boundary conditions. In addition, they improved the accuracy of the complex Young's modulus measurement of the composite Oberst beam by performing curve fitting on the frequency

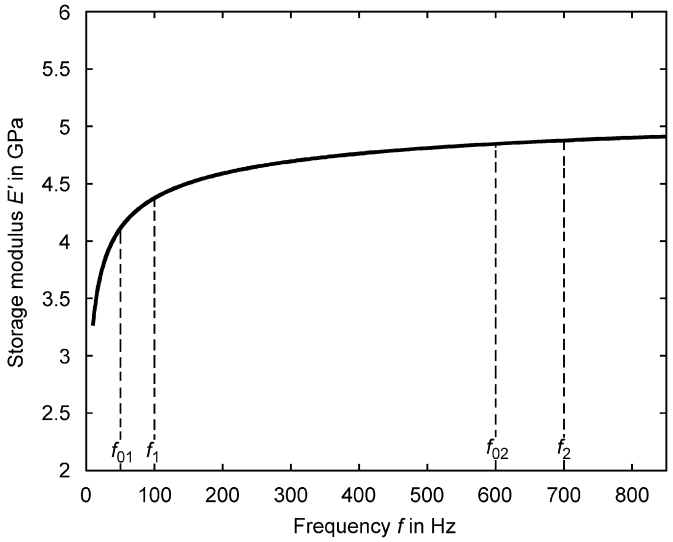

Fig. 1. Storage modulus vs. frequency diagram of a base beam material.

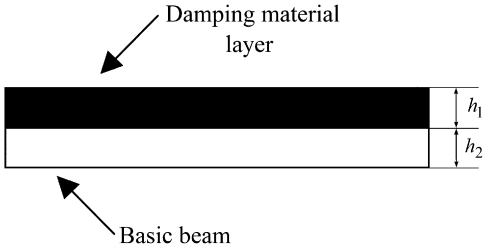

Fig. 2. Oberst beam schematic.

response functions (FRF) obtained by using white noise excitations. However, in order for this technique to yield accurate results, the beam needs to be fully covered with damping material. In addition, the material properties can only be determined near modal frequencies.

This paper proposes a modified Oberst beam technique unhindered by the above restrictions. The main difference between the modified method and the Oberst technique is that the modified approach utilizes non-parametric COE and LS data analysis methods rather than conventional analysis for estimating the complex moduli of the base beam and the composite beam. Though this work presents application only to unconstrained layer systems with one damping layer, a similar process can be applied to multi-layer unconstrained or constrained layer systems.

In the paper, the basic Oberst beam theory is briefly introduced. The modified Oberst beam technique is developed. Finally simulated and experimental results obtained on styrene–butadiene rubber (SBR) material and a very soft high-damping adhesive material are presented and discussed.

2. Theory

2.1. Oberst equation and extraction of layer properties

As shown in Fig. 2, an Oberst beam system consists of one base beam and one damping layer. The base beam provides the necessary stiffness, and the viscoelastic material layer dissipates as much vibration energy as possible. The combined system will be referred to as the "composite beam" for the rest of this paper.

The effective properties of the composite system can be determined in many ways. Oberst's equation is derived in Ref. [15]:

$$\frac{E^*_{\text{eff}} I_{\text{eff}}}{E^*_1 I_1} = 1 + e^* h^3 + 3(1+h)^2 \frac{e^* h}{1 + e^* h}, \tag{1}$$

where the complex modulus ratio e^* and thickness ratio h are defined as

$$e^* = \frac{E^*_2}{E^*_1}, \quad h = \frac{h_2}{h_1}. \tag{2}$$

E_{eff}^* is the effective complex modulus of the combined system, I_{eff}, the effective second moment of inertia, E_2^*, the complex modulus of the damping layer material, E_1^*, the complex modulus of the base beam material, I_1, the second moment of the base beam, and h_1 and h_2 are the thicknesses of the base beam and damping layer, respectively. The complex modulus E^* can be written in the form of $E'(1+i\eta)$ with η representing the loss factor, or, alternatively, as $E'+iE''$ with E' and E'' called the storage modulus (or real modulus) and loss modulus, respectively. The cross-sectional areas of the base beam and the layer are rectangular with the same width b. Accordingly, I_1 is $bh_1^3/12$, I_2 is $bh_2^3/12$ and I_{eff} is $b(h_1+h_2)^3/12$.

The Oberst beam equation can be used in reverse to obtain the complex modulus of the layer material. Let the bending stiffness ratio $\alpha^* = E_{\text{eff}}^* I_{\text{eff}}/(E_1^* I_1)$, and rearrange Eq. (1) into a quadratic for e^*:

$$h^4 (e^*)^2 + (4h + 6h^2 + 4h^3 - \alpha^* h) e^* + 1 - \alpha^* = 0. \tag{3}$$

Solving the above equation for e^* results in

$$e^* = \frac{-\beta^* h \pm \sqrt{(\beta^* h)^2 - 4h^4 (1 - \alpha^*)}}{2h^4}, \tag{4}$$

where

$$\beta^* = 4 + 6h + 4h^2 + 4h^3 - \alpha^*. \tag{5}$$

Then the complex modulus of the layer material can be calculated:

$$E_2^* = \frac{E_1^*}{2h_2^3} \left(\sqrt{(\beta^*)^2 - 4h_2^2 (1 - \alpha^*)} - \beta^* \right). \tag{6}$$

Eq. (6) is the governing equation used to obtain the complex modulus of the non-stiff layer materials in the experiments.

2.2. Oberst beam technique

The Oberst beam analysis makes use of a cantilever beam configuration. Aluminum is the typical material for the base beam because it can be easily machined according to test requirements. Aluminum has a very low loss factor and its storage modulus is fairly constant over the frequency range of most interest for vibration control, 10–2000 Hz. Therefore, the complex modulus of aluminum can be considered as a constant, and this simplifies the layer property extraction process.

The technique consists of three steps. First, modal testing is performed to determine the resonance frequencies of the base beam, which are then used to calculate its Young's modulus:

$$E_1 = \frac{48 \rho_1 \pi^2 L^4 f_{0j}^2}{h_1^2 \lambda_j^4}, \tag{7}$$

where ρ_1 is the density of the base beam, L is the cantilever length, f_{0j} is the jth resonance frequency and λ_j is the corresponding characteristic eigenvalue [18]. Second, the resonance frequencies are obtained for the

composite beam and they are used to calculate the effective storage modulus:

$$E'_{\text{eff}} = \frac{48\rho_{\text{eff}}\pi^2 L^4 f_j^2}{(h_1+h_2)^2\lambda_j^4}, \tag{8}$$

where f_j is the jth resonance frequency of the composite beam and ρ_{eff} is the effective density, i.e. $(\rho_1 h_1 + \rho_2 h_2)/(h_1+h_2)$. The effective loss factor $\eta_{\text{eff},j}$ is estimated for the composite beam using the half-power bandwidth method. Finally the bending stiffness ratio α^* can be computed as

$$\alpha^*_{\text{Traditional}} = \frac{\rho_1 h_1 + \rho_2 h_2}{\rho_1 h_1}\left(\frac{f_j}{f_{0j}}\right)^2 (1 + \mathrm{i}\eta_{\text{eff},j}) \tag{9}$$

and Eqs. (5) and (6) are used to compute the complex modulus of the layer material.

2.3. Modified Oberst beam technique

Though the Oberst beam method has been commonly used in practice, there are several disadvantages associated with it: (1) the complex modulus can only be evaluated at resonance frequencies, (2) the base beam should be fully covered with the layer material and (3) exact mathematical boundary conditions are often difficult to mimic in the laboratory.

Moreover, an assumption has been made in using the conventional technique regarding Young's modulus behavior of the base beam. As shown in Eqs. (7) and (8), the Young's modulus of the base beam is evaluated at f_{0j}, and the effective complex modulus is obtained at f_j. If one wants to calculate the complex modulus of the layer material at frequency f_j, the modulus properties of the base beam at *exactly* f_j should be used. Therefore, the standard method implicitly assumes that the complex moduli of the base beam are the same or very close at frequencies f_{0j} and f_j. This is a good assumption if the base beam material is aluminum whose Young's modulus does not vary much with frequency. However, as will be shown in Section 5, to improve the estimation accuracy of the layer modulus, materials whose moduli are more frequency-dependent could be used as the base beam material, and the above assumption can lead to large errors when the base beam modulus varies significantly with the frequency.

A modified Oberst beam technique for evaluating damping layer material properties is proposed. The bending stiffness of the base beam and the effective bending stiffness of the composite beam can be determined as

$$E_1^* I_1 = \frac{\omega^2 \rho_1 A_1}{(k_1^*)^4}, \quad E_{\text{eff}}^* I_{\text{eff}} = \frac{\omega^2 \rho_{\text{eff}} A_{\text{eff}}}{(k_{\text{eff}}^*)^4}, \tag{10}$$

where k_1^* and k_{eff}^* are wavenumbers for the base beam and composite beam, respectively, which are estimated by the COE or LS method. Then the bending stiffness ratio α^* is calculated as

$$\alpha^*_{\text{Modified}} = \frac{\rho_1 h_1 + \rho_2 h_2}{\rho_1 h_1}\left(\frac{k_1^*}{k_{\text{eff}}^*}\right)^4. \tag{11}$$

Finally the complex modulus of the layer is obtained by using Eqs. (5) and (6).

It can be seen that the difference between the conventional technique and the modified one is the approach to obtaining the bending stiffness ratio α^*. While the conventional Oberst beam technique uses conventional modal testing methods, the modified technique exploits the non-parametric COE and LS methods.

Since the COE and LS methods are used for estimation, the modulus-related properties can be evaluated at any frequency. Moreover, the COE and LS methods are boundary condition independent. Therefore, the base beam need not be completely covered by the layer, and one only needs to take measurements in the covered area to determine the effective properties.

2.4. Very soft material case

If the layer material is very soft relative to the base beam material, i.e., $|E_2^*| \ll |E_1^*|$ or $|e^*| \ll 1$, and the thickness ratio h is not large, which consequently results in a small $|e^*|h$, the Oberst equation, Eq. (1), can be approximated as

$$\frac{E_{\text{eff}}^* I_{\text{eff}}}{E_1^* I_1} = 1 + e^*(3h + 6h^2 + 4h^3) \tag{12}$$

or

$$E_{\text{eff}}^* I_{\text{eff}} = E_1^* I_1 + \frac{3h + 6h^2 + 4h^3}{h^3} E_2^* I_2. \tag{13}$$

The complex modulus of the layer material can then be extracted:

$$E_2^* = \frac{(1+h)^3 E_{\text{eff}}^* - E_1^*}{3h + 6h^2 + 4h^3}. \tag{14}$$

Moreover, if the base-beam material has very low damping, i.e., E_1^* is almost real-valued, and the layer is a very soft material with a large loss factor, an approximated simple formula can be used to estimate the effective loss factor of the composite beam [3]:

$$\eta_{\text{eff}} = 3h(1+h)^2 \frac{E_2'}{E_1} \eta_2. \tag{15}$$

3. Experimental setup

Fig. 3 shows the setup for the experiments. The test composite beam consists of a layer of the soft layer material whose properties are of interest, and a stiff base beam. A function generator (Hewlett Packard 33120A) generates a source sinusoidal signal at a desired frequency. The signal is then augmented by an amplifier (MB Dynamics SS250) and fed into a shaker (MB Dynamics PM50A), which is used to excite the test beam. The vibration velocity wave field of the beam is measured by a Polytec PSV-200 laser vibrometer, and delivered to the vibrometer controller as the Channel B signal. The channel A signal is a phase reference signal that is measured by an accelerometer (PCB Piezotronics 353B17) placed on the clamp and amplified by a signal conditioner (PCB Piezotronics 482A16). PSV-200 software is used for data acquisition. Matlab is used to execute the Wave Coefficients algorithm to estimate the effective complex modulus of the composite beam, and then extract the properties of the layer material.

4. Experimental results

4.1. Complex modulus of the base beam material PMMA

In the experiments, the base beam was the PMMA beam used by Liao and Wells for testing in Ref. [12]. Fig. 4 shows the complex modulus estimation results obtained by Liao and Wells using the COE and the LS methods. Note that the wicket plot process [19–20] had been used to filter out random errors in the original experimental data. As discussed in Ref. [12], the vibrometer system had a resonance frequency close to 350 Hz, near which the vibration velocity measurement quality was compromised. This led to the exclusion of most data points near 350 Hz after the wicket process.

Also shown in Fig. 4 is a fit curve (dashed line) based on the fractional derivative model [19] commonly used for complex modulus of viscoelastic materials:

$$E_1(f) = \frac{0.9206(1 + \text{i}0.8866) + 10.4654(1 + 0.0275)(\text{i}f)^{0.3533}}{1 + 1.9285(\text{i}f)^{0.3533}} \quad \text{(GPa)}. \tag{16}$$

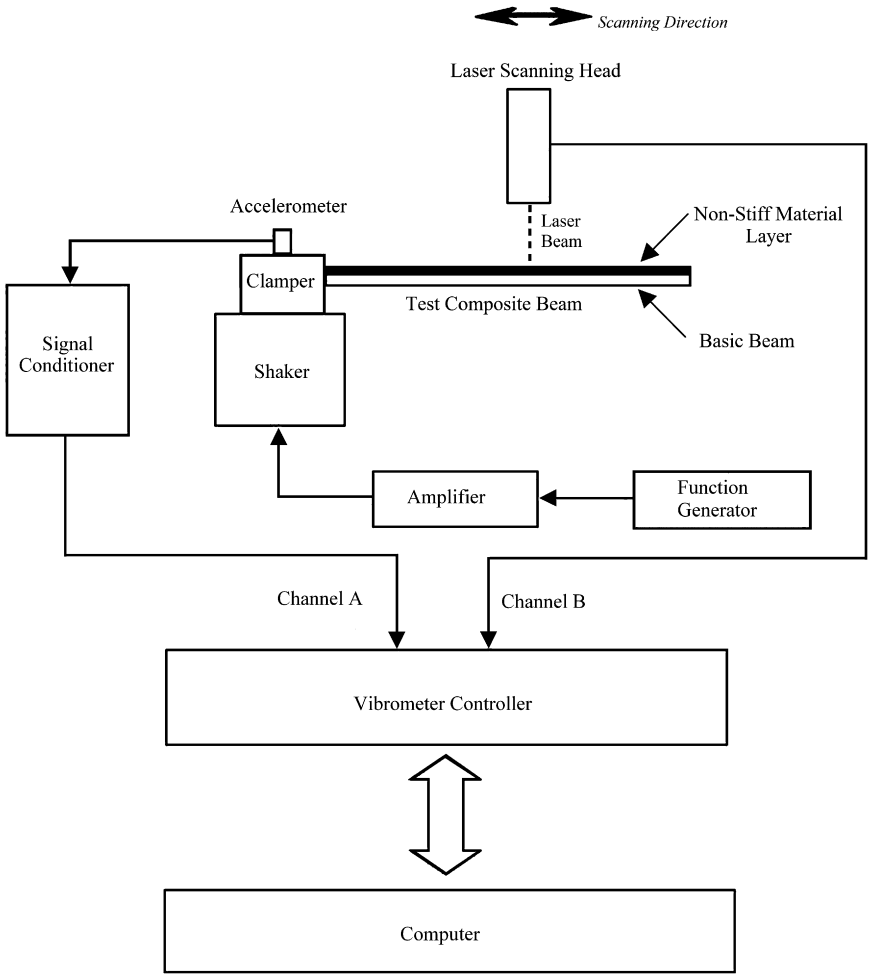

Fig. 3. Experimental setup.

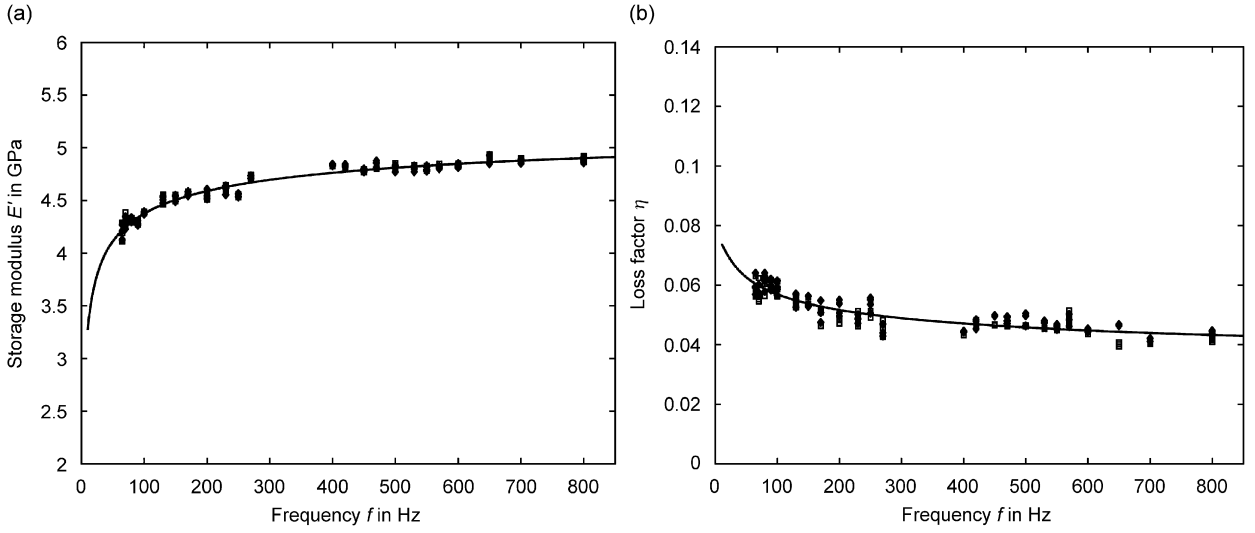

Fig. 4. Complex modulus vs. frequency f for polymethyl methacrylate (PMMA). (a) Storage modulus E'; (b) loss factor η. ◆, wave coefficients (COE) method results; □, least squares (LS) method results. ⋯, fit results from Eq. (16). Near 22.5 °C.

4.2. SBR layer results

Experiments were performed on a SBR sample of undisclosed composition using the modified Oberst beam technique. SBR, also called GR-S or Buna-S, is a copolymer of styrene and butadiene and is the most commonly used type of synthetic rubber. The base beam was the PMMA beam used for testing in Ref. [12]. It had thickness 4.42 mm, width 20 mm and density 1183.6 kg/m^3. The SBR layer had a thickness of 3 mm, a width of 20 mm and a density of 1464.5 kg/m^3. The cross sections for the base beam and layer were both rectangular. The outer 320 mm of the PMMA beam was covered by the SBR material. The test composite beam was clamped at one end and free at the other with a cantilever length of 340 mm. The test temperature was near 22.5 °C. The system reached steady state after a waiting time of approximately 20 min. The maximum amplitude of the vibration velocity of the test beam was controlled to be close to but lower than 50 mm/s. The velocity measurement resolution of the vibrometer was 3 μm/s. The sampling frequency was 5120 Hz and the frequency resolution was 0.625 Hz. The data analysis utilized two different measurement points combinations for each frequency; and each combination had 8–10 measurement points.

First the effective complex modulus of the composite beam was estimated by using the COE method. Then the SBR layer properties were extracted from the effective properties by using Eq. (6). The complex modulus of the PMMA base beam was calculated from Eq. (16) (the curve-fit PMMA complex modulus expression obtained from experimental results). Fig. 5 shows the complex modulus results of the SBR layer after the wicket process. The storage modulus of the SBR increases from about 0.17 GPa at 80 Hz to 0.23 GPa at 650 Hz, and then drops to 0.22 GPa at 850 Hz. The loss factor increases from around 0.18 at 80 Hz to 0.3 at 850 Hz.

4.3. SBR result discussions

SBR rubber was first developed in the United States and Germany (Buna-S) during World War II when important supplies of natural rubber were cut off. Since then, many experiments have been performed to evaluate its viscoelastic properties.

Fletcher and Schofield [21] found that at a temperature of 20 °C the storage Young's modulus for a Buna-S sample was around 0.311 GPa at testing frequencies 20–60 Hz, with a loss factor of about 0.163. Moyal and Fletcher [22] did further testing on two GR-S samples. One was a GR-S compound with nominally 60° Shore hardness and the other was a GR-S natural rubber 50/50 compound of nominal hardness 50° Shore. For the first sample, its storage Young's modulus and loss factor were found to be about 0.216 GPa and 0.208, respectively, while for the other sample, they were around 0.120 GPa and 0.137. These authors used half-power bandwidth and logarithmic methods to determine the loss factors. The results were obtained at frequency about 110 Hz. Payne [23] gave 0.087 GPa and 0.22 as reference values for the storage shear modulus and loss factor of SBR, with no frequency specified. Since the Poisson's ratio for SBR is very close to 0.5 [23], the corresponding storage Young's modulus is 0.261 GPa. Mancke and Ferry [24] performed thorough testing of cross-linked SBR, and Table 1 shows some of their measured storage shear moduli and loss factors. For comparison purpose, the storage Young's modulus in the table was obtained by multiplying Mancke and Ferry's storage shear modulus by a factor of 3 (assuming a Poisson's ratio of 0.5). Another detailed test was performed by Jones [5] on a SBR sample using the conventional modal testing technique and a Van Oort beam configuration [25], i.e., two symmetrical unconstrained layers on both sides of the base beam, at 8 different temperatures. Complex modulus information was extracted from the loss factors of the composite beam estimated by the half-power bandwidth method, and the resonance frequency ratios between the resonance frequencies of the base beam and those of the composite beam. Table 2 shows some of the results obtained by Jones.

Since different SBR samples were used by the above researchers, and they were manufactured by different companies at different times, there is a high probability that the compositions of the samples were different. The techniques or equipment, or both, used by the researchers were also different. These all would lead to differences in the complex modulus results.

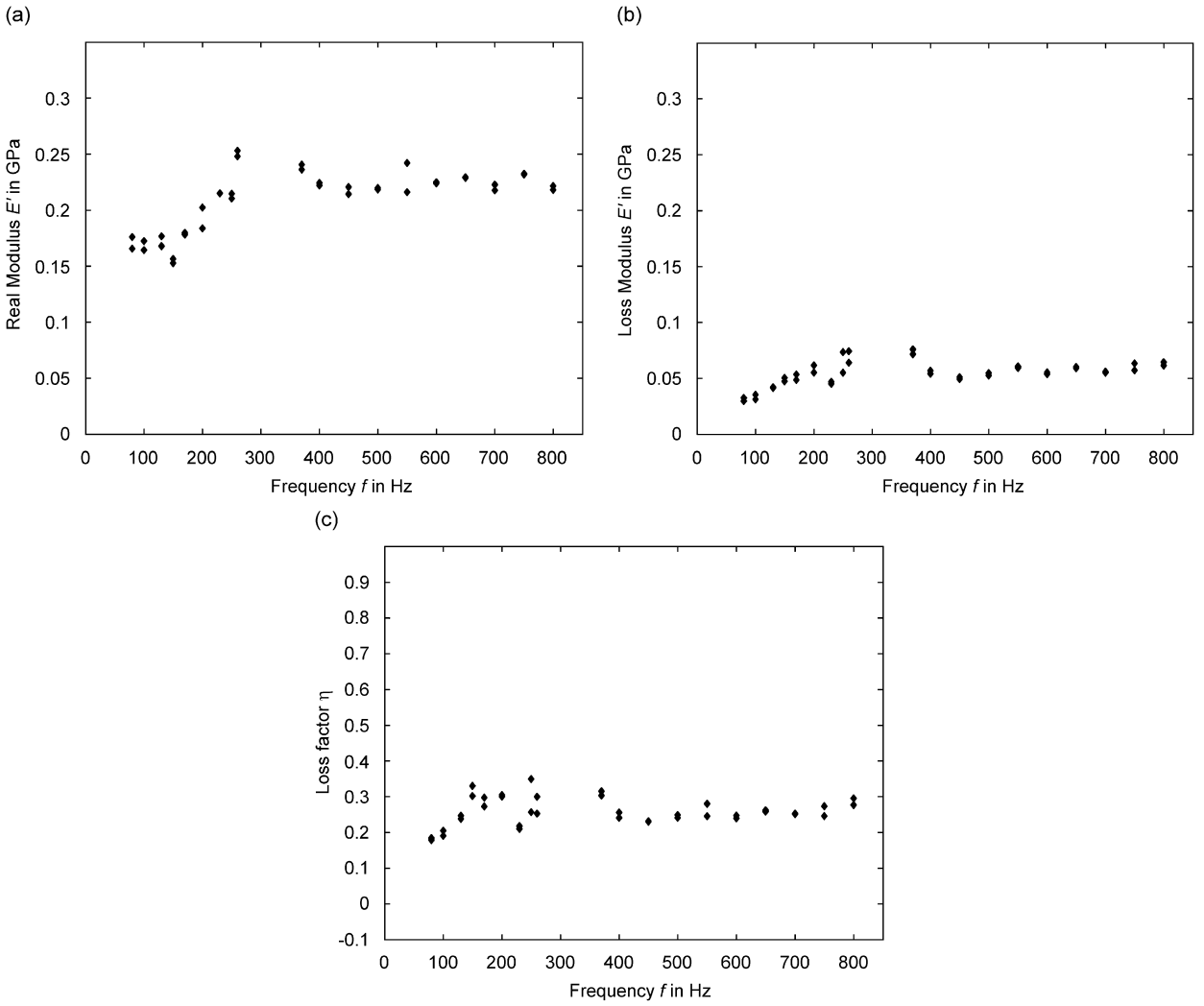

Fig. 5. Complex modulus E vs. frequency f for styrene–butadiene rubber (SBR). (a) Storage modulus E'; (b) loss modulus E''; (c) loss factor η. Near 22.5 °C.

Table 1
Storage shear modulus, storage modulus and loss factor of very lightly cross-linked styrene-butadiene rubber (SBR) (temperature 25 °C) by Mancke and Ferry [24]

Frequency (Hz)	Storage shear modulus (GPa)	Storage modulus[a] (GPa)	Loss factor
5	0.058	0.173	0.166
16	0.066	0.198	0.145
50	0.072	0.217	0.132
159	0.081	0.244	0.126
503	0.089	0.267	0.141
1592	0.102	0.306	0.191

[a]The storage Young's modulus was calculated by multiplying the storage shear modulus by a factor of 3 since the SBR has a Poisson's ratio very close to 0.5.

Table 2
Experimental complex modulus of styrene–butadiene rubber (SBR) by Jones [5]

Temperature (°C)	f_{0n}[a] (Hz)	f_n[b] (Hz)	η_n[c]	Storage modulus E' (GPa)	Loss factor
14.4	126.6	118.4	0.222	0.3835	0.338
	355.0	352.1	0.323	0.4577	0.464
	696.2	715.4	0.206	0.6296	0.264
26.7	125.8	89.3	0.143	0.1167	0.352
	352.8	263.7	0.172	0.1733	0.371

[a] f_{0n}, resonance frequency of the base beam.
[b] f_n, resonance frequency of the composite beam.
[c] η_n, loss factor of the composite beam.

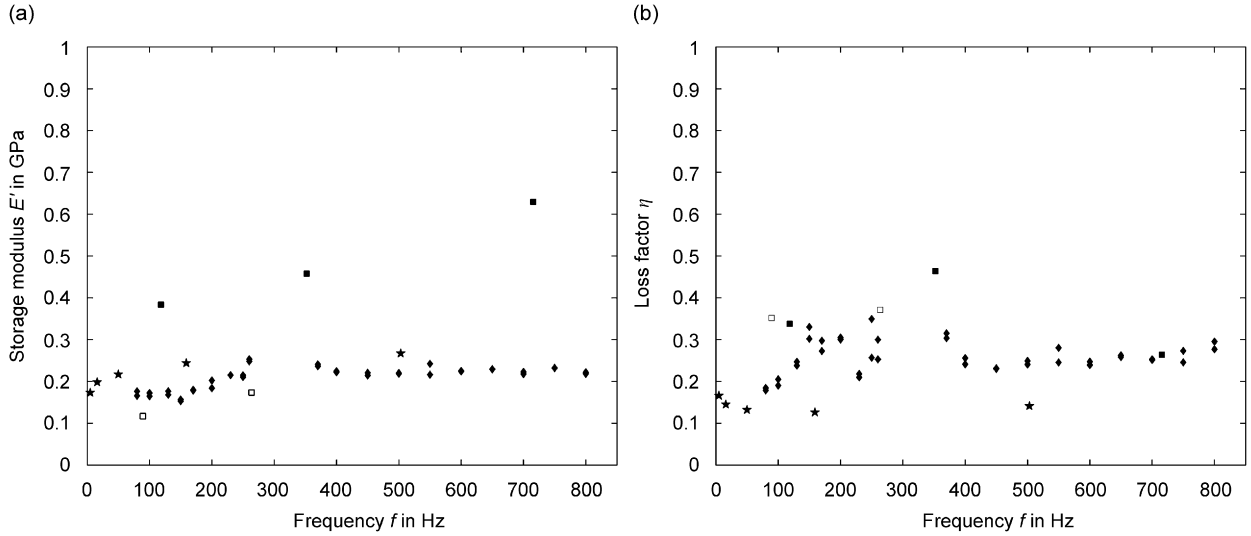

Fig. 6. Complex modulus E vs. frequency f for styrene–butadiene rubber (SBR). (a) Storage modulus E'; (b) loss factor η. ◆, wave coefficients (COE) method results (near 22.5 °C); ★, Mancke and Ferry's results (at 25 °C) [24]; ■, Jones' results (at 14.4 °C) [5]; □, Jones' results [5] (at 26.7 °C).

However, the measurements show that for a general SBR, the storage Young's modulus is between 0.1 and 0.3 GPa and the loss factor falls between 0.1 and 0.4, at frequencies ranging from 5 to 1600 Hz, with temperatures around 20–25 °C.

For comparison purposes, the SBR results obtained in this work, Mancke and Ferry's results, and Jones' results are plotted in Fig. 6. As the figure shows, the storage modulus and loss factor results, obtained by the COE and LS methods with the aid of unconstrained layer theories, are in those ranges. Moreover, except the near-350 Hz area the storage modulus and loss factor curves are quite smooth in the frequency range of interest, and this is usually an indication of good measurement quality. In addition, when the frequency is greater than 80 Hz, overall the curves increase as frequency increases and this is in agreement with the patterns shown in Tables 1 and 2.

One final note is that measurements show that the SBR sample tested in this work is undoubtedly different from normal SBR rubbers. This sample has a density of 1464.5 kg/m^3, while typical values are 930–1200 kg/m^3 [23]. It is possible that the manufacturer added other materials into the raw SBR material to enhance its performance for various applications.

5. Uncertainty analysis

5.1. Uncertainty analysis

Uncertainty analysis was performed to study the effects of experimental configurations on the complex modulus measurement accuracy. The uncertainty analysis was based on Eq. (14), the approximation to the exact layer modulus equation, valid for $|e^*h| \ll 1$. In the experiments in Section 4, e^*h was less than 0.05 for the SBR measurements in the frequency range of interest. It has been confirmed by simulations that the approximation Eq. (14) can yield quite accurate results in situations where the thickness ratio is small and the base beam is much stiffer than the layer. Therefore, the uncertainty analysis can be carried out on Eq. (14) without any appreciable loss of accuracy.

In the analysis, only uncertainties related to complex modulus estimation methods were examined, which include uncertainties in the storage modulus, loss modulus and loss factor measurements.

Recall that if the result R is a function of independent variables $t_1, t_2, t_3, \ldots, t_n$, i.e. $R = R(t_1, t_2, t_3, \ldots, t_n)$, the root sum of squares (RSS) uncertainty [26] in the result R is given as

$$\Delta R = \left[\left(\frac{\partial R}{\partial t_1}\Delta t_1\right)^2 + \left(\frac{\partial R}{\partial t_2}\Delta t_2\right)^2 + \cdots + \left(\frac{\partial R}{\partial t_n}\Delta t_n\right)^2\right]^{1/2}.$$

Following this formula, the uncertainty equations for Eq. (14) can be written as follows:

$$\Delta E'_2 = \frac{\sqrt{(1+h)^6(\Delta E'_{\text{eff}})^2 + (\Delta E'_1)^2}}{3h + 6h^2 + 4h^3} \tag{17}$$

and

$$\Delta E''_2 = \frac{\sqrt{(1+h)^6(\Delta E''_{\text{eff}})^2 + (\Delta E''_1)^2}}{3h + 6h^2 + 4h^3}, \tag{18}$$

where $\Delta E'_2$ and $\Delta E''_2$ are the uncertainties for the storage modulus and loss modulus of the layer, respectively. $\Delta E'_{\text{eff}}$ and $\Delta E'_{\text{eff}}$ represent the uncertainties for the storage modulus and loss modulus of the composite beam, and $\Delta E'_1$ and $\Delta E'_1$ are the uncertainties for the storage modulus and loss modulus of the base PMMA beam.

In terms of storage modulus and loss factor uncertainties, Eq. (18) can be rewritten as

$$\Delta E''_2 = \frac{\sqrt{(1+h)^6[\eta^2_{\text{eff}}(\Delta E'_{\text{eff}})^2 + (E'_{\text{eff}})^2\Delta\eta^2_{\text{eff}}] + \eta^2_1(\Delta E'_1)^2 + (E'_1)^2\Delta\eta^2_1}}{3h + 6h^2 + 4h^3}. \tag{19}$$

For analysis purposes, if one introduces the normalized storage modulus percentage uncertainty Δe^{Nor} such that $\Delta E' = E'\Delta e^{\text{Nor}}$. Eqs. (18) and (19) can be rewritten as

$$\Delta E'_2 = \frac{\sqrt{(1+h)^6(E'_{\text{eff}})^2(\Delta e^{\text{Nor}}_{\text{eff}})^2 + (E'_1)^2(\Delta e^{\text{Nor}}_1)^2}}{3h + 6h^2 + 4h^3}, \tag{20}$$

$$\Delta E''_2 = \frac{\sqrt{(1+h)^6(E'_{\text{eff}})^2[\eta^2_{\text{eff}}(\Delta e^{\text{Nor}}_{\text{eff}})^2 + \Delta\eta^2_{\text{eff}}] + (E'_1)^2[\eta^2_1(\Delta e^{\text{Nor}}_1)^2 + \Delta\eta^2_1]}}{3h + 6h^2 + 4h^3}, \tag{21}$$

For the uncertainty analysis, the complex modulus estimation uncertainties were assumed to be 1% for the storage modulus and 0.005 for the loss factor; in other words, $\Delta e^{\text{Nor}}_{\text{eff}} = \Delta e^{\text{Nor}}_1 = 0.01$ and $\Delta\eta^{\text{Nor}}_{\text{eff}} = \Delta\eta^{\text{Nor}}_1 = 0.005$. These are close to the actual uncertainties in experiments for the complex modulus [12]. The analysis was then carried out as follows: first, the SBR complex modulus results were fit to second-order polynomials to approximate the modulus properties in the frequency ranges tested. Then the effective complex modulus of the composite beam was calculated from the Oberst equation Eq. (1), using the curve-fit

properties and base PMMA beam properties as given by Eq. (16). Finally, the uncertainties for the layer modulus E_2 were computed by Eqs. (20) and (21).

5.2. Uncertainty analysis for SBR results

For the analysis, the SBR experimental moduli were curve-fitted by second-order polynomials, represented by the two solid lines in Fig. 7. The two polynomials were $E' = -3.38 \times 10^{-7} f^2 + 3.64 \times 10^{-4} f + 1.36 \times 10^{-1}$ GPa for the storage modulus and $E'' = -1.09 \times 10^{-7} f^2 + 1.18 \times 10^{-4} f - 2.99 \times 10^{-2}$ GPa for the loss modulus.

Fig. 8 shows the percentage uncertainties for different thickness ratios between the layer and base beam for the SBR layer case. The percentage uncertainty was obtained by multiplying 100 with the ratio between the uncertainty calculated from Eq. (20) or (21) and its corresponding theoretical storage modulus or loss modulus for the layer. The actual thickness ratio in the SBR experiments was 0.679. For this ratio, the analysis shows the percentage uncertainty is less than 10% for the storage modulus and between 10% and 15% for the loss modulus. This is in good agreement with the experiment results shown in Fig. 5, which appear to form very smooth curves.

Fig. 8 shows that as the thickness ratio increases, the percentage uncertainties decrease. If the thickness ratio is larger than one, the percentage uncertainties are both less than 8% in the frequency range of interest, which implies good estimation quality.

5.3. Uncertainty analysis discussions

As shown in Fig. 8, the uncertainties in the storage modulus and loss modulus measurements decrease as the thickness ratio increases. At frequencies ranging from 70 to 850 Hz, when the thickness ratio increases from 0.5 to 2, the storage modulus uncertainty drops from about 10% to less than 2% and the loss modulus uncertainty falls from around 20% to 3%.

Therefore, the uncertainty analysis shows that the estimation accuracy can be improved by increasing the thickness ratio between the layer and base beam. It also can be achieved by selecting a base beam material with a smaller modulus magnitude (thus, to attain more contributions from the layer material in the effective properties). For example, the base beam can be made of polypropylene (PP), whose complex modulus magnitude lies between 2 and 3 GPa at frequencies ranging from 50 to 1000 Hz near 22 °C [11], instead of PMMA, whose complex modulus magnitude is between 4 and 5 GPa in the frequency range.

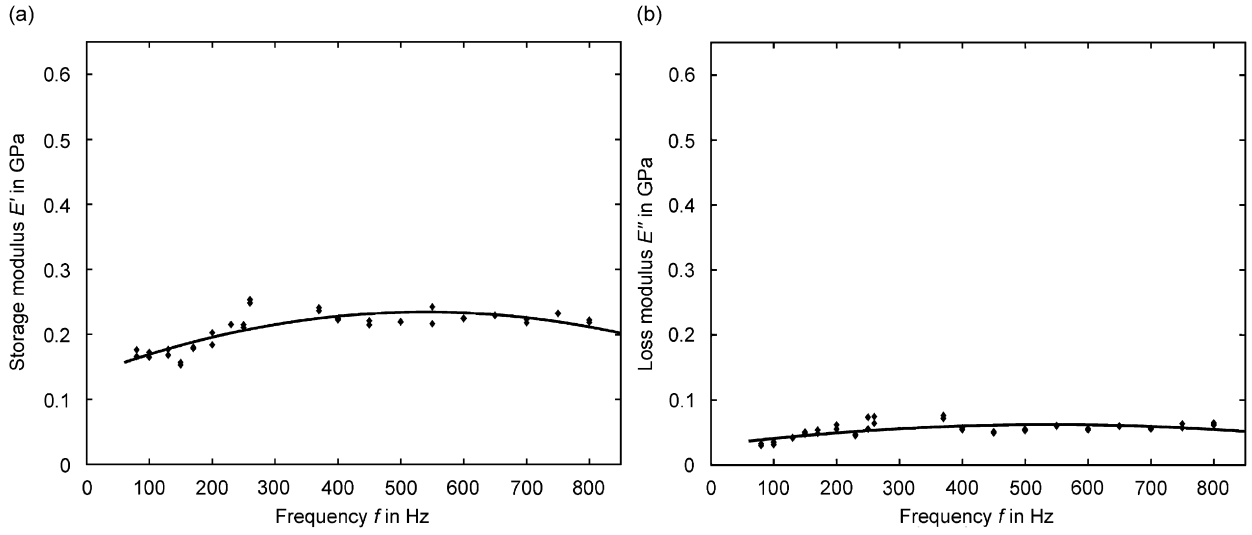

Fig. 7. Complex modulus vs. frequency f for styrene-butadiene rubber (SBR). (a) Storage modulus, E'; (b) loss modulus, E''. ◆, wave coefficients (COE) method results; —, second-order polynomial fit.

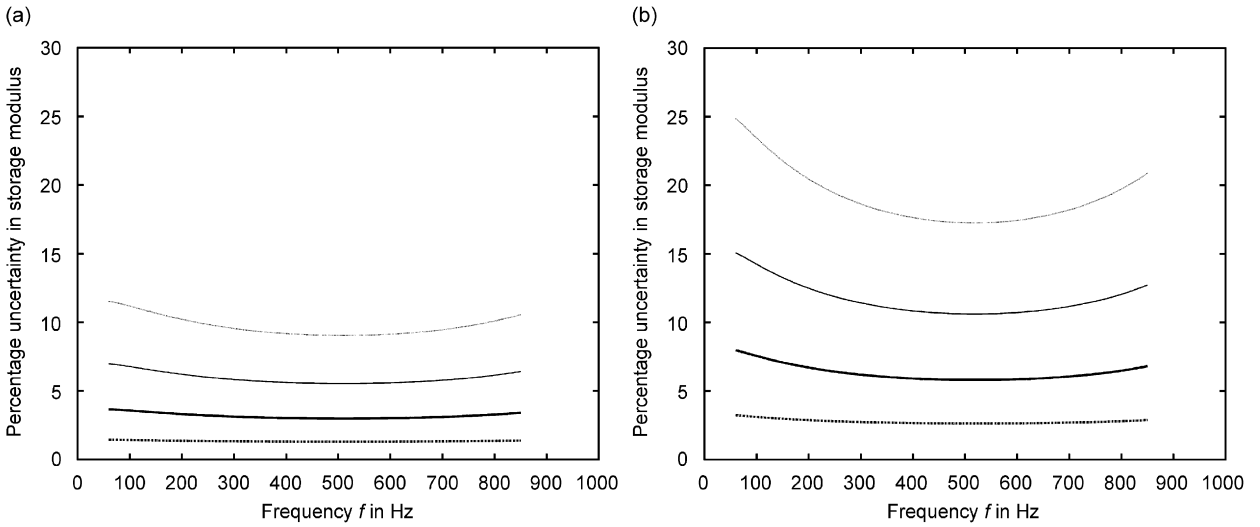

Fig. 8. Percentage uncertainties vs. frequency f for styrene–butadiene rubber (SBR) with different thickness ratios. (a) In storage modulus, $\Delta E'$; (b) in loss modulus, $\Delta E''$. ⋯⋯, $h_2/h_1 = 0.5$; —, $h_2/h_1 = 0.679$ (ratio in experiments); ▬, $h_2/h_1 = 1$; ▮▮▮▮▮▮▮▮, $h_2/h_1 = 2$.

6. Conclusions

In this paper, a modified Oberst beam technique is proposed to measure the complex modulus of materials that are not stiff enough to be tested directly using beam configurations. The material can be coated on a base beam. The complex modulus of the base beam and effective complex modulus of the composite beam are measured using the COE and LS methods. Then the complex modulus of the layer can be extracted using layer theories.

The modified approach has several advantages over the conventional Oberst beam technique: the layer properties can be evaluated at any frequency, the base beam can be partially covered, and it does not require the complex modulus of the base beam to be fairly constant around the resonance frequencies analyzed to yield accurate results.

The method was applied to a styrene–butadiene rubber (SBR) sample that was coated on a PMMA base beam to attain an Oberst beam configuration. The results are in good agreement with those in the literature.

Uncertainty analysis on the layer property extraction shows that the estimation accuracy can be improved by selecting a base beam material with a small complex modulus magnitude, or increasing the thickness ratio between the layer and base beam.

References

[1] B.E. Read, G.D. Dean, *The Determination of Dynamic Properties of Polymers and Composites*, Wiley, New York, 1978.
[2] J.D. Ferry, *Viscoelastic Properties of Polymers*, Wiley, New York, 1980.
[3] L. Cremer, M. Heckl, B.A.T. Petersson, *Structure-Borne Sound*, Springer, Berlin, 2005.
[4] A.Ya. Malkin, A.A. Askadsky, V.V. Kovriga, A.E. Chalykh, *Experimental Methods of Polymer Physics*, MIR Publishers, Moscow, 1983.
[5] D.I.G. Jones, *Handbook of Viscoelastic Vibration Damping*, Wiley, New York, 2001.
[6] S.O. Oyadiji, G.R. Tomlinson, Determination of the complex moduli of viscoelastic structural elements by resonance and non-resonance methods, *Journal of Sound and Vibration* 101 (1985) 277–298.
[7] S. Sim, K.J. Kim, A method to determine the complex modulus and Poisson's ratio of viscoelastic materials for FEM applications, *Journal of Sound and Vibration* 141 (1990) 71–82.
[8] T. Pritz, Transfer function method for investigating the complex modulus of acoustic materials: rod-like specimens, *Journal of Sound and Vibration* 81 (1982) 359–376.
[9] G. Kurtze, K. Tamm, S. Vogel, Pilot experiments to the flexible shafts damping on corners, *Acustica* 5 (1955) 223–233 (in German).
[10] A.J. Hull, D.A. Hurdis, A parameter estimation method for the flexural wave properties of a beam, *Journal of Sound and Vibration* 262 (2003) 187–197.

[11] L. Hillström, M. Mossberg, B. Lundberg, Identification of complex modulus from measured strains on an axially impacted bar using least squares, *Journal of Sound and Vibration* 230 (2000) 689–707.
[12] Y. Liao, V. Wells, Estimation of complex modulus using wave coefficients, *Journal of Sound and Vibration* 295 (2006) 165–193.
[13] A.D. Nashif, D.I.G. Jones, J.P. Henderson, *Vibration Damping*, Wiley, New York, 1985.
[14] R. Plunkett, Measurement of damping, ASME Annual Meeting: Structure Damping, 1959, pp. 117–131 (Section 5).
[15] H. Oberst, K. Frankenfeld, On the damping of bending vibrations on thin sheet metal by firmly bonded coatings (in German), *Acustica* 2 (1952) 181–194.
[16] D. Ross, E.E. Ungar, E.M. Kerwin Jr., Damping of plate flexural vibrations by means of viscoelastic laminae, ASME Annual Meeting: Structure Damping, 1959, pp. 49–88 (Section 5).
[17] J.L. Wojtowicki, L. Jaouen, R. Panneton, New approach for the measurement of damping properties of materials using the Oberst beam, *Journal of Scientific Instruments* 75 (2004) 2569–2574.
[18] D.J. Inman, *Engineering Vibration*, Prentice-Hall, Englewood Cliffs, NJ, 2001.
[19] L.C. Rogers, Operators and fractional derivatives for viscoelastic constitutive equations, *Journal of Rheology* 27 (1983) 351–372.
[20] D.I.G. Jones, On temperature-frequency analysis of polymer dynamic mechanical behaviour, *Journal of Sound and Vibration* 140 (1990) 85–102.
[21] W.P. Fletcher, J.R. Schofield, The variation with temperature of the dynamic properties of rubber and synthetic rubber-like materials, *Journal of Scientific Instruments* 21 (1944) 193–198.
[22] J.E. Moyal, W.P. Fletcher, Free and forced vibration methods in the measurement of the dynamic properties of rubbers, *Journal of Scientific Instruments* 22 (1945) 167–170.
[23] A.R. Payne, The physical properties of polymers, *Society of Chemical Industry Monograph* 5 (1959) 273.
[24] R.G. Mancke, J.D. Ferry, Dynamic mechanical properties of cross-linked rubbers. IV. Dicumyl Peroxide vulcanizates of Styrene-Butadiene rubber, *Transactions of the Society of Rheology* 12 (1968) 335–350.
[25] W.P. Van Oort, A method for the measurement of dynamic mechanical properties of small samples of plastic material, *Microtecnic VIII* 5 (1952) 246.
[26] S.J. Kline, F.A. McClintock, Describing uncertainties in single sample experiments, *Mechanical Engineering* 75 (1953) 3–8.